J Comput Aided Mol Des (2013) 27:723–738
DOI 10.1007/s10822-013-9673-3

Molecular dynamics simulation and linear interaction energy study of D-Glu-based inhibitors of the MurD ligase

Andrej Perdih · Gerhard Wolber · Tom Solmajer

Received: 5 February 2013 / Accepted: 6 August 2013 / Published online: 30 August 2013

Abstract The biosynthetic pathway of the bacterial peptidoglycan, where MurD is an enzyme involved at the intracellular stage of its construction, represents a collection of highly selective macromolecular targets for novel antibacterial drug design. In this study as part of our investigation of the MurD bacterial target two recently discovered classes of the MurD ligase inhibitors were investigated resulting from the lead optimization phases of the *N*-sulfonamide D-Glu MurD inhibitors. Molecular dynamics simulations, based on novel structural data, in conjunction with the linear interaction energy (LIE) method suggested the transferability of our previously obtained LIE coefficients to further D-Glu based classes of MurD inhibitors. Analysis of the observed dynamical behavior of these compounds in the MurD active site was supported by static drug design techniques. These results complement the current knowledge of the MurD inhibitory mechanism and provide valuable support for the D-Glu paradigm of the inhibitor design.

Keywords Molecular dynamics (MD) simulations · Linear interaction energy (LIE) method · Structure-based pharmacophore models · MurD ligase · Antibacterial agents · Drug design

Electronic supplementary material The online version of this article (doi:10.1007/s10822-013-9673-3) contains supplementary material, which is available to authorized users.

A. Perdih (✉) · T. Solmajer
National Institute of Chemistry, Hajdrihova 19, 1001 Ljubljana, Slovenia
e-mail: andrej.perdih@ki.si

A. Perdih · G. Wolber
Institute of Pharmacy, Freie Universität Berlin, Königin Luise-Strasse 2+4, 14195 Berlin, Germany

Introduction

The increased bacterial resistance to numerous antibiotics present today has made the discovery of novel efficacious antibacterial agents imperative and is stimulating both academic and industrial research efforts [1]. In this process, novel previously unexploited targets are being considered [2]. The inhibition of bacterial peptidoglycan biosynthesis is traditionally accepted as one of the optimal approaches to tackle this problem with respect to selective toxicity and efficacy [3]. Peptidoglycan formation outlines a complex multistage process divided into early stages of intracellular assembly of UDP-MurNAc pentapeptide followed by a translocation step on the extracellular side and its final incorporation into the nascent biopolymer molecule [3]. If properly constructed, peptidoglycan provides the necessary rigidity, flexibility and strength to prokaryotic cell to withstand high internal osmotic pressure [3].

The family of bacterial Mur ligases—MurC, MurD, MurE and MurF—is involved in the intracellular phase of peptidoglycan assembly, catalyzing the synthesis of a peptide moiety by consecutive addition of L-Ala, D-Glu, *meso*-DAP (or L-Lys) and D-Ala-D-Ala to the starting precursor [4]. The three-domain structure of the Mur ligase family comprises an N-terminal domain primarily responsible for binding of the precursor substrate, a central domain bearing resemblance to the ATP-binding domains of several ATP- or GTP-ases and a C-terminal domain which is hypothesized to be involved in binding the incoming condensing amino acids [4].

All Mur ligases are presumed to act through an analogous sequential enzymatic mechanism, as corroborated by structural [5], biochemical [6, 7] and computational studies [8]. In the proposed mechanism, the bound UDP-precursor substrate initially reacts with the ATP molecule to yield the

acylphosphate intermediate, which provides a tetrahedral reaction intermediate following the addition of the incoming amino acid. Finally, the dissociation of the phosphate group results in a new UDP-precursor elongated for the condensed amino acid [5–8].

MurD (UDP-*N*-acetylmuramoyl-L-alanine:D-glutamate ligase) enzyme (Fig. 1) is the second member in the bacterial Mur ligase series. It catalyzes the incorporation of the D-glutamate to the cytoplasmic intermediate UDP-*N*-acetyl-muramoyl-L-alanine (UMA), concomitant with the degradation of ATP to ADP and P_i (Fig. 2) [5]. Detailed structural research of the MurD ligase resulted in the identification of different protein conformations with respect to the position of the C-terminal domain [9]. The conformational closure of MurD has been computationally investigated in great detail providing a dynamic model of this dynamic process [10, 11].

Previous research of this enzyme as potential drug target resulted in the design of several MurD inhibitors [12] as the transition state analogues based on the hypothetical structure of the enzyme's tetrahedral reaction intermediate [13]. Following the initial success of this approach, several low-molecular-weight analogues of the MurD tetrahedral intermediate were discovered and further structurally characterized. One of the discovered classes-*N*-sulphonamide derivatives of the D-glutamic acid—are depicted schematically in Fig. 2 by a generalized structure [14]. The binding of this series of the *N*-substituted sulphonamide D-Glu-based inhibitors was also computationally investigated by binding free energies calculation using linear interaction energy (LIE) method, which revealed a principal role of non-polar van der Waals interactions as the inhibitor binding main driving force in the molecular recognition [15].

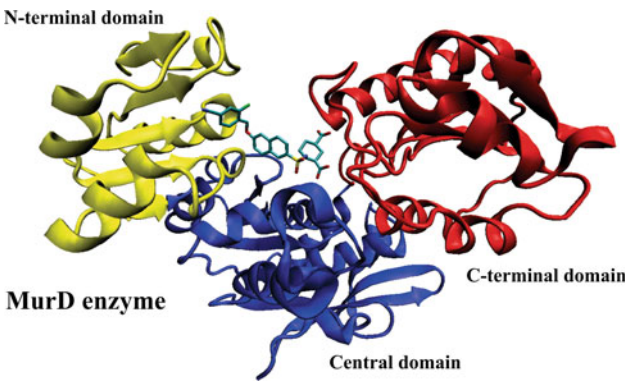

Fig. 1 Crystal structure of the MurD enzyme complexed with a representative of newly discovered classes of MurD inhibitor—compound **4** used in our computational studies (PDB code: 2XPC). N-terminal domain is denoted in *yellow*, central domain in *blue* and C-terminal domain in *red*. Bound conformation of the inhibitor **4** is located between the UDP-substrate (UMA) and the D-Glu binding site [18]

The optimization of the *N*-substituted sulfonamide D-Glu-based inhibitors was principally performed in two directions schematically depicted in Fig. 2. Firstly, the search for novel moieties, which could replace the *N*-substituted sulfonamide resulted in two successful examples: D-glutamic acid-based inhibitors incorporating either 5-benzylidenethiazolidine-2,4-dione (compound **2**) [16] or 5-benzylidenethiazolidin-4-one (compound **3**) [17]. For compounds **2** and **3** their binding modes were determined experimentally using protein crystallography [17]. An alternative optimization route 2 was performed by replacing the D-Glu moiety with several rigid substitutes (e.g. cyclohexane- or benzene-based dicarboxylic acids) while concurrently preserving the substituted sulphonamide moiety of the initial *N*-substituted sulphonamide D-Glu-based inhibitors **1**. This strategy took into account the results of the virtual screening experiments in which several inhibitors with rigidly substituted D-Glu replacements were identified [19]. For compound **4** with incorporated cyclohexane-1,3-dicarboxyl moiety a crystal structure was determined (Fig. 1) showing a perfect analogy of the ligand binding mode obtained in the crystal structures of the D-Glu series of inhibitors (see Figure **1S** for the structural alignment of novel MurD structures) [16–18].

The aim of this study as part of our ongoing investigation of the MurD ligase enzyme is to apply our previously used computational approach in studying MurD ligase inhibition and molecular recognition [15] to analyze the geometric and energetic behavior of these two novel chemical classes of D-Glu-based inhibitors using available structural information on their binding [16–18]. Molecular dynamics (MD) simulations using experimental structural data were performed to observe the dynamical behavior of these compounds in the MurD active site. In conjunction with an established LIE method [20, 21] estimates of binding free energy values were calculated taking our previous findings into account [15]. These results were further supported by conventional drug design computational techniques. This deeper insight into molecular recognition of these compounds will form a good foundation for establishing novel guidelines in subsequent optimization steps.

Methods and computational strategies

Preparation of molecular system for MD simulation

Our study was based on novel experimentally solved structures of the MurD enzyme representing the starting coordinates for our molecular dynamics simulations, that were retrieved from the Protein Data Bank (PDB codes: 2X5O, 2Y68 and 2XPC) [16–18]. Computational resources

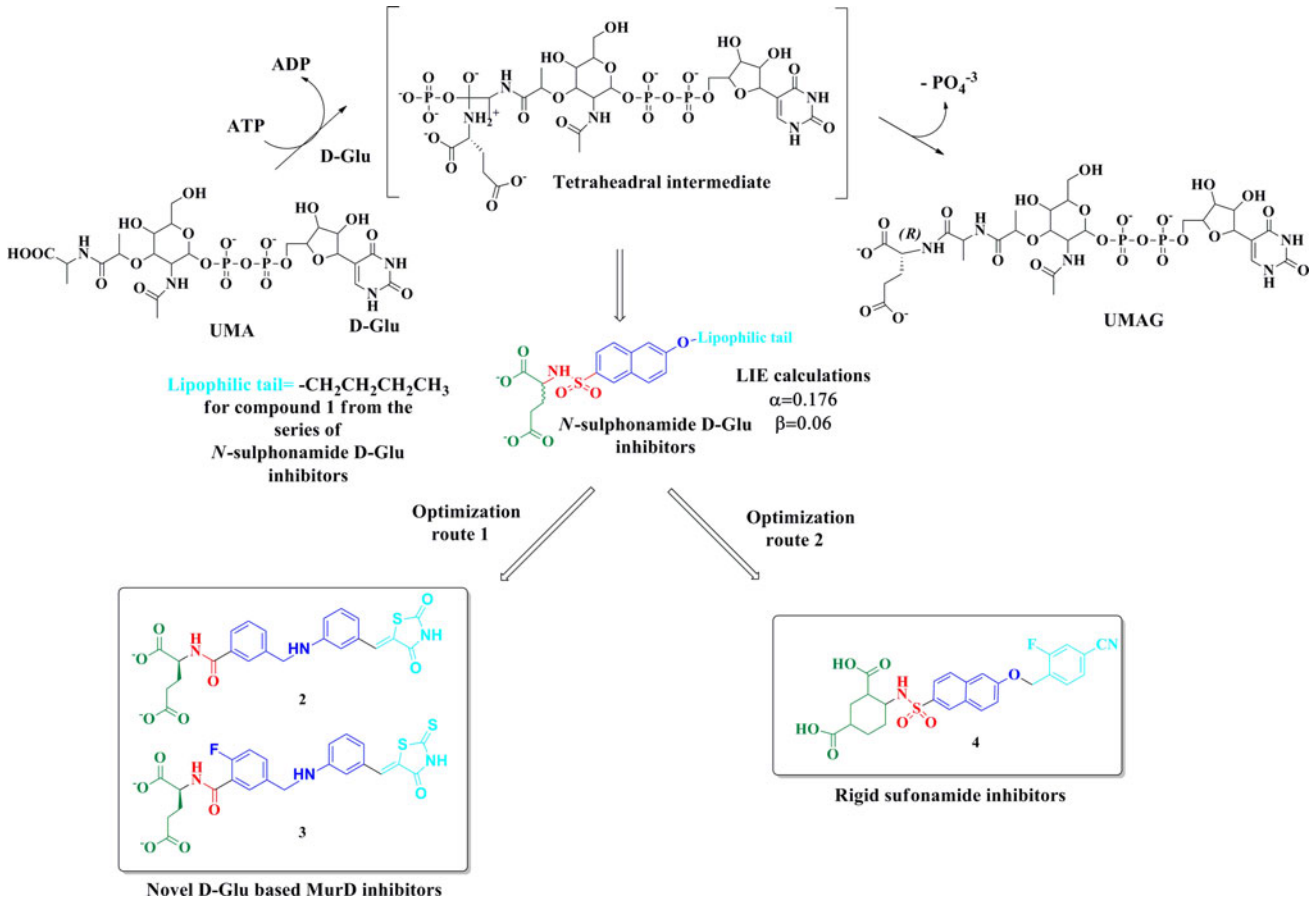

Fig. 2 Reaction catalyzed by the MurD enzyme and the structure of the tetrahedral reaction intermediate which comprised a starting point for the discovery of *N*-sulphonyl-glutamic acid inhibitors which were then optimized through two different routes leading to the discovery of novel chemical classes of D-Glu containing inhibitors **2**–**4** of MurD ligase [16–18]. Compound **1** of this series with the butyl lipophilic tail will be used for comparison with the novel results [15]

of the Laboratory of Biocomputing and Bioinformatics at the National Institute of Chemistry in Ljubljana, Slovenia, were exploited in our free energy studies. Preparation of the initial structures, as well as molecular dynamics simulations and free energy calculations, were performed with the Q program [22] developed by Åqvist and co-workers using AMBER force field [23] (see Figure **2S** for the graphical outline of all steps of the LIE study).

The empirical force field parameters for all inhibitors **2**–**4** were developed in a similar matter as for the inhibitor **1** used in our previous study [15]. Atomic parameters (charges and atom types) for the MurD carbamylated residue Lys198 (KCX198) also present in all novel crystal structures were taken from our previous computational investigations [15]. In order to determine partial atomic charges, all newly simulated ligands **2**–**4** were extracted from their complexes and hydrogen atoms were added. The obtained structures were fully optimized at the Hartree–Fock (HF) level of theory using a 6-31G(d) basis set and followed by a subsequent vibrational analysis using Gaussian 09 program [24]. The vibrational frequencies analysis showed the absence of imaginary frequencies in all calculations [15]. The RESP charge-fitting procedure reproduced the calculated electrostatic potential (ESP) surrounding the inhibitors **2**–**4** [25]. Partial charges of chemically equivalent atoms were restricted to the same value. Standard van der Waals parameters were applied. Missing stretching, bending, dihedral and improper dihedral parameters required for the complete description of the inhibitors were taken from the Generalized AMBER Force Field (GAFF) [23]. In all cases where the exact parameters were not available in GAFF the chemically most analogous GAFF parameters were used. Determined partial RESP charges and assigned atom types for inhibitors **2**–**4** are listed in the Supplementary material.

Crystal waters in the PDB structures were removed and the ligand's bound states **2**–**4** were prepared by constructing a sphere of TIP3P [26] water molecules with a radius of 25 Å centered on the C14 atom (compounds **2**, **3**) or O33 atom (compound **4**). Analogously, the ligand's free-state was prepared by constructing a sphere of TIP3P water molecules around the ligand, again with a radius of 25 Å

and centered on the C14 atom (compounds **2**, **3**) or O33 atom (compound **4**). Protonation of the ionizable amino acid residues was assigned by the following previously utilized rules [15]: side chains of Asp, Glu and KCX residues located within 22 Å of the sphere center were treated as negatively charged. Similarly, side chains of Lys and Arg residues were treated as positively charged. In the area between 22 and 25 Å away from the sphere center, the ionizable residues were mostly treated as neutral entities. In salt bridges, both of the interacting partners were charged. Histidine residues located within 22 Å of the sphere center were assigned their protonation pattern in the last stage to approach the electroneutrality of the system. In our MD simulations, the following residues were considered charged [15]: Arg (32, 37, 52, 100, 186, 200, 302, 371, 425), Lys (45, 115, 319, 348, 420), Asp (2, 35, 44, 59, 94, 182, 185, 317, 346, 372, 417), Glu (51, 90, 96, 157, 164, 181, 388, 423, 428), His (53, 78, 183, 301). The sum of their total charges together with the KCX residue with a total charge of −1 and the inhibitor's total charge of −2 required the addition of 5 sodium ions in the bound state to make the system electroneutral. In the free state, two sodium ions were included for this purpose. Topology and coordinate files necessary for the initiation of molecular dynamics simulations were generated using the Qprep5 subprogram of the Q program [22].

Molecular dynamics simulations details

Molecular ensembles that served for the calculation of interaction energies and subsequent evaluation of binding free energies were generated by MD simulations using the Qdyn subprogram of the Q suite [22]. During the MD simulations surface constraint all atoms solvent (SCAAS) spherical boundary conditions, which mimic the infinite aqueous solution, were used [27]. Protein atoms located outside of the 25 Å sphere boundary were restrained to their coordinates using harmonic constraints. Non-bonded interactions of these atoms were turned off. Non-bonded interactions were assessed for distances under 10 Å. The local reaction field (LRF) method was used to treat long-range electrostatics for distances beyond the 10 Å cut-off value [28]. A restraining harmonic potential applying a force constant of 100 kcal/mol $Å^2$ was applied to the position of the C14 atom (compounds **2**, **3**) or O33 atom (compound **4**) for all investigated ligands in their free state. The position of sodium ions was restrained by a 75 kcal/mol $Å^2$ flat-bottom harmonic potential that was set to zero for distances less than 21.5 Å from the center of the simulation sphere. These potentials were applied to prevent diffusion of inhibitors and sodium ions toward the edge of the simulation sphere.

Molecular systems were subjected to a simulation procedure used in our previous study [15]: first optimized by series of two 30,000- and 20,000-step MD simulations at 5 K with a step size of 0.005 and 0.01 fs, respectively. In systems representing the bound state, the coordinates of protein and ligand heavy atoms were constrained, allowing only for water relaxation, as opposed to the free state, in which the inhibitor atoms were allowed to move freely. In succeeding stages the systems were relaxed at 5 K by a series of four 20,000- and one 50,000-step simulations with increasing integration step size (step size prolongation program: 0.01, 0.04, 0.1, 0.3 and 1 fs). Subsequent heating of the simulated system from 5 to 298 K was performed by a series of six simulations using a 1 fs integration step (temperature heating steps: 50, 100, 150, 200, 250, 298 K), comprising 300–330 ps of total simulation time. A 200 ps MD simulation at 298 K using a 2 fs step size with the SHAKE algorithm applied to bonds involving hydrogen atoms yielded the starting structure for the production phase.

Production MD trajectories yielded molecular ensembles with number of molecules, volume, and temperature of the system fixed [29]. The 2 fs integration step used was coupled with SHAKE algorithm applied to bonds involving hydrogen atoms. The energy of the system was sampled every 10 steps. Production runs of 5 ns were initiated from 4 starting configurations (obtained by the heating protocols of 300, 310, 320, 330 ps length which resulted in different configurations, respectively). This resulted in 20 ns of total production run for each of the investigated systems. A caveat must be stated that despite different staring structures were used in the MD production runs some degree of correlations could have still remained causing potentially not complete independence of these simulations.

To evaluate the binding free energies of the selected moieties, molecules **2**–**4** were decomposed into four regions [15], as shown schematically in the division scheme available in the Supplementary material. The first moiety consisted of the glutamate residue (or it rigid cyclohexane moiety in compound **4**) without the amino group; the second included atoms of the amide or sulphonamide functional group. A biphenyl system connected by an aliphatic chain or naphthalene ring and the bridging oxygen encompassed the third moiety. The fourth moiety consisted either of the 5-benzylidenethiazolidine-2,4-dione (compound **2**) [16] or the 5-benzylidenethiazolidin-4-one scaffold (compound **3**) [17] or the remaining lipophilic 2-fluoro-4-cianobenzyl substituent present in compound **4** [18]. Visualization and analysis of the geometry parameters (atom distances, RMS fluctuations etc.) of the production trajectories were performed using VMD program [30]. The measured distances were first measured between selected atom pairs and obtained data was subsequently exported

for statistical analysis. Standard deviations (SD) were calculated from four 5 ns MD production run simulations which were initiated from four different starting configurations. The analysis of the interaction energies was performed using Qfeb utility available within the program Q [22].

Linear interaction energy (LIE) calculations

Linear interaction energy approach was developed by Åqvist et al. and it represents a rapid established computational method of evaluating binding free energies. LIE is based on a modified linear response approximation for electrostatics and empirical term treating the non-polar interactions [20, 21]. In LIE approach only MD simulations of two physical states—the bound and free state of an investigated ligand—have to be performed, which reduces computational expense considerably compared with other methods for binding free energy calculations [31]. The thermodynamic cycle forming the base of the LIE calculations is graphically presented in Figure **3S** of the Supplementary material. The core of the LIE method states that binding free energy can be calculated as a free energy difference of the process when a ligand is transferred from either aqueous solution (denoted as free state W) or solvated receptor binding site (denoted as bound state P) to vacuum state (1)[20].

$$\Delta G_{binding} = \Delta G^{W}_{decoupling} - \Delta G^{P}_{decoupling} \quad (1)$$

According to LIE methodology solvation free energies can expressed as (2):

$$\Delta G^{Q}_{solvation} = -\Delta G^{Q}_{decoupling} = \alpha\left\langle V^{vdW}_{L-Q}\right\rangle + \beta\left\langle V^{ES}_{L-Q}\right\rangle \quad (2)$$

where $\langle V^{vdW}_{L-Q}\rangle$ and $\langle V^{ES}_{L-Q}\rangle$ represent van der Waals (vdW) and electrostatic (ES) interaction energy between ligand L and its surrounding Q—either aqueous solution W or solvated binding site P—averaged over the molecular ensemble of MD-generated configurations. By combining Eqs. (2) and (3), binding free energy can be obtained with a full LIE formalism as follows:

$$\Delta G_{binding} = \alpha\left(\left\langle V^{vdW}_{L-P}\right\rangle - \left\langle V^{vdW}_{L-W}\right\rangle\right) + \beta\left(\left\langle V^{ES}_{L-P}\right\rangle - \left\langle V^{ES}_{L-W}\right\rangle\right) \quad (3)$$

The values of empirical LIE coefficients α and β used in this study were taken from our previous study of the *N*-sulphonyl-D-Glu MurD inhibitors [15]. The coefficients were obtained by generating a RMSD function between the interaction energies expressed as a function of both empirical coefficients α and β and experimental binding free energies over the series of eight *N*-sulphonyl-D-Glu MurD inhibitors with determined inhibition activity in micromolar range. The minimum of this function at 0.19 kcal/mol corresponds to the optimal values of LIE coefficients $\alpha = 0.176$ and $\beta = 0.06$ [15]. The value of the van der Waals α LIE coefficient was in line with previously reported values observed in a variety of enzymatic systems [32–35]. Also, in the literature several LIE studies on various other enzymatic systems (e.g. protein kinases) were published determining a similar value for the electrostatic LIE parameter β as obtained in our study [15, 34, 35]. Molecular mechanics force fields allow the interaction energy to be decomposed into contributions of particular atom groups or moieties present in molecule [36]. Thus, the binding free energies of selected moieties can be explicitly evaluated within the LIE formalism which is important for the evaluation of the moieties' individual contribution to binding. This, however, represents an important information in the drug design optimization stage.

Results and discussion

Geometrical properties of the ligands during the MD simulations

In all performed MD simulations two physical states were simulated independently. They are depicted schematically in Fig. 3 for the case of compound **4**. The compounds free state comprised the inhibitor molecule immersed into a sphere of water molecules. Two sodium atoms were introduced to keep the system total charge neutral. The bound state was represented by the experimentally determined conformation of the MurD-ligand complex with the constructed water sphere that described the water environment surroundings and additional five sodium ions that kept the system electroneutral. Animations of the calculated MD trajectory of the new classes of compounds **2** and **4** in the bound state are available in the Supplementary material.

The production phase 20 ns trajectories, comprised from 4 5 ns MD simulations of the bound state of systems **2–4,** were first analyzed in terms of the several geometrical parameters that correspond to the stability assessment of the individual ligand, in the MurD binding site. Root mean square distance (RMSD) time-dependent graphs show a conformational deviation between the MD-generated conformations **2–4** and the X-ray conformations that were calculated with all atoms taken into consideration (Fig. 4). SD providing a quantitative benchmark of the measured H-bond distance fluctuations were calculated from four 5 ns MD production runs initiated from 4 different starting structures. The obtained RSMD averages of 0.8 ± 0.2 Å for compound **2**, 0.9 ± 0.1 Å for compound **3**, and 0.9 ± 0.1 Å for compound **4** indicate a very

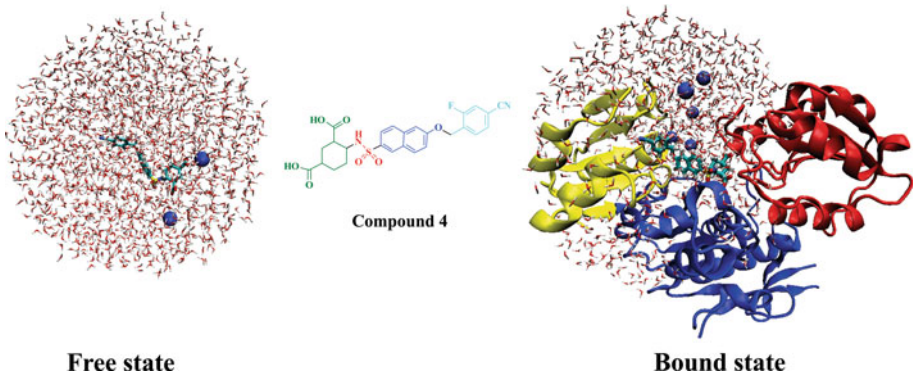

Fig. 3 Free (*left*) and bound states (*right*) systems of compound **4** prepared for the MD simulation studies. *Blue spheres* indicate sodium atoms that were included to make the system electroneutral. The constructed sphere of water molecules is depicted in *red*. Domains of the MurD enzyme are colored using the same colored scheme as in Fig. 1

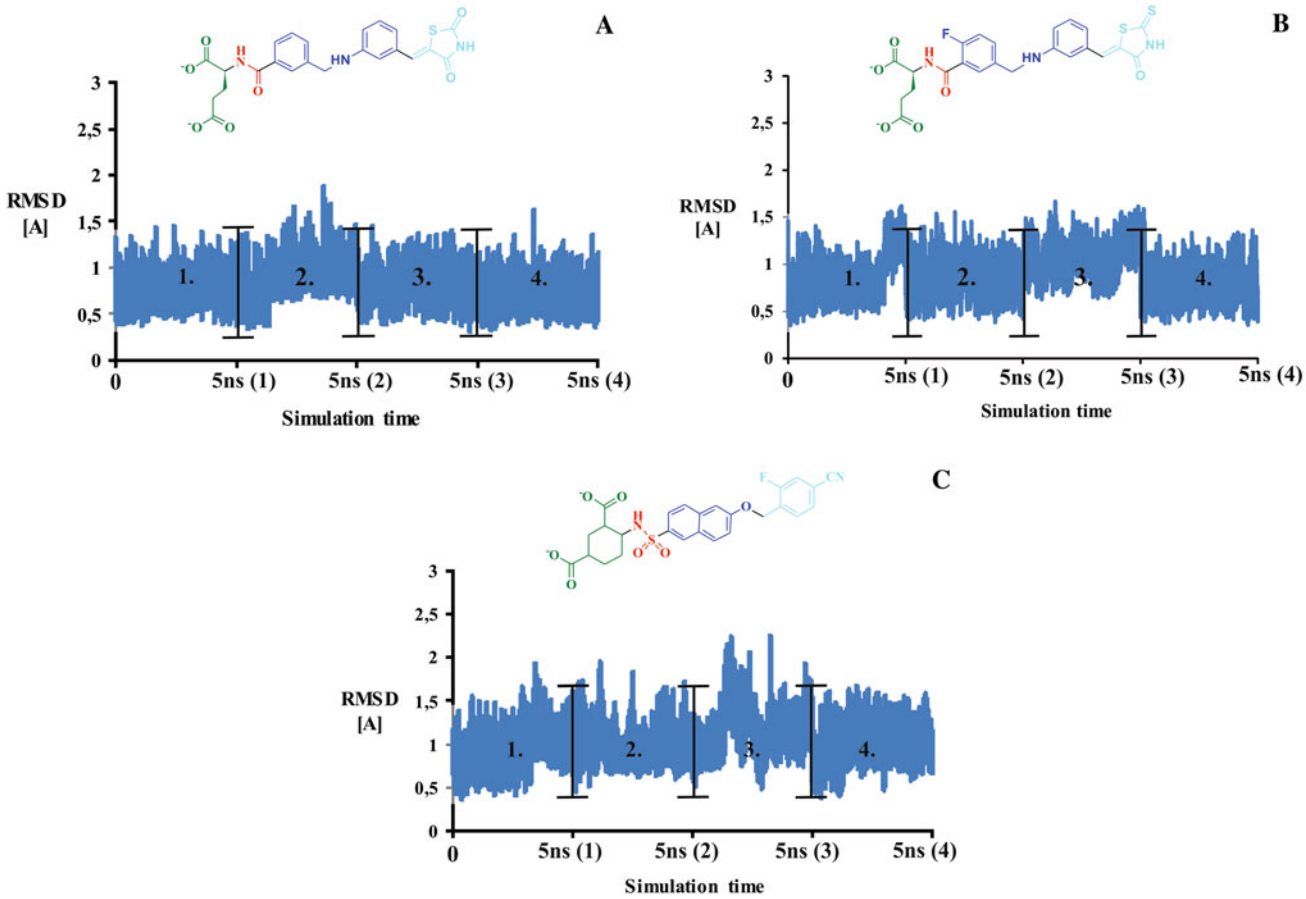

Fig. 4 Time-dependent RMSD graphs showing the deviation of the conformations of the simulated MurD inhibitors—compounds **2** (**a**), **3** (**b**), **4** (**c**) generated during the MD simulation from the template X-ray conformations [16–18]. All atoms were taken into account. Bars indicate boundaries between four 5 ns MD production runs staring from different starting configurations

stable conformation with little deviation of the generated conformations from the original X-ray conformation. RMSD graphs also show a uniform distribution of MD-generated conformations for all structures. Both structures **2** and **3** contain a classic D-Glu moiety, which in contrast to L-Glu [15] provides a more uniform conformation also in this class of D-Glu based inhibitors. Further inspection of the overall conformational behavior can also be seen in the generated movie animation for compound **2** (see Supp. Information). This is an expected observation as this enzyme is fully optimized to recognize and incorporate exclusively D-Glu amino acid to the bound UDP-substrate [4]. The cyclohexane moiety with two carboxylic acids at the 1,3 positions also enabled a stable binding conformation, validating that the rigidization optimization route 2 (Fig. 2) [18] represents a reasonable substitution alternative to the established D-Glu paradigm. Further inspection of this behavior can also be seen in the

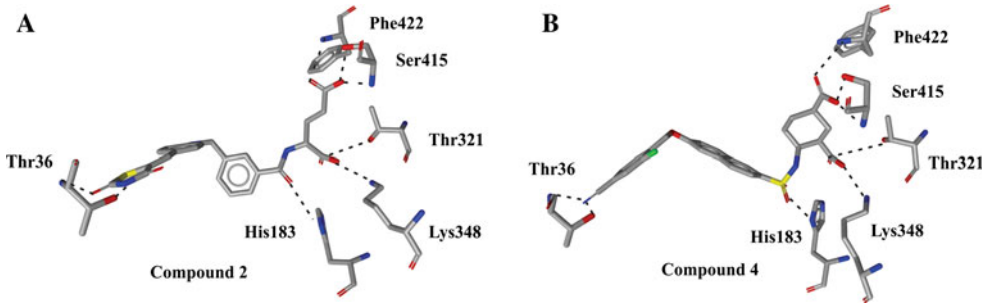

Fig. 5 Depicted monitored bond distances of the D-Glu based inhibitor (**2**) and its rigid D-Glu surrogate (**4**) as revealed in the experimental X-ray structures 2Y68 and 2XPC respectively [16, 18]. Similar binding pattern was observed also for compound **3** [17] Interaction between Thr321 and compounds proceed via connecting conserved water molecule not shown in this figure [14, 15, 18]

generated movie animation for compound **4** (see Supplementary material).

Further geometrical parameters under investigation were the selected distances, some of them hydrogen bonds, observed in the determined X-ray complexes [14, 16–18] important for inhibitor molecular recognition. Time-dependence graphs of all monitored distances are available in the Supplementary material (Figures **4S–6S**). In addition, results of all monitored distances for each simulation run separately are available in the Supplementary material (Tables **4S.1–4S.3** and **5S.1–5S.3**) and do not deviate substantially from the overall average values discussed. Figure 5 depicts the monitored distances as observed in the experimental X-ray structures for both compound classes (**A** D-Glu compound **2** and **B** rigid alternative **4**) [14, 16–18]. The obtained average distances from four 5 ns simulation runs are gathered in Table 1. The interactions between Thr321 and Lys348 and α-D-Glu carboxylate (or its corresponding carboxylate group on the rigid substitute of compound **4**) and between Ser415 and Phe422 residues and γ-D-Glu carboxylate (or its corresponding carboxylate group on the rigid substitute of compound **4**), were included in the distance monitoring. To enable a better comparison with the previous series of N-sulphony D-Glu MurD inhibitors in Table 1 as well as in all other Tables 2, 3, 4 and 5 the results from our initial study are included for the selected *N*-sulphonyl MurD inhibitor **1** containing the butyl hydrophobic tail (Fig. 2) [15].

The measured average distances demonstrated little deviation in the length of the observed hydrogen bond distances between MurD residues and γ-carboxylate (or corresponding carboxylate on the compound **4** rigid D-Glu substitute) in all compounds. These results are fully in line with the results of our previous computational study [15]. The H-bond distances between γ-carboxylate and backbone nitrogen of Ser415 are between 2.8 and 3.3 Å whereas the values to side chain oxygen of Ser415 fluctuate from 2.6 to 3.0 Å. H-bond distances between the side chain of nitrogen Phe422 and γ-carboxylate are in the interval between 2.90 and 3.60 Å. Favorable values of the hydrogen bonds throughout the four 5-ns MD simulations, signify the importance of the γ-carboxylate for successful molecular recognition and binding of both novel series.

The α-carboxylate moiety interacts with two MurD residues: directly with Lys348 residue and indirectly with Thr321 via connecting conserved water molecule [16–18]. The measured distances to the side chain nitrogen of Lys348 have values between 2.8 and 3.3 Å. Expectedly, larger average distances of the interaction with Thr321 between 3.1 and 3.9 Å for the novel compounds were

Table 1 Average distances between compounds **1–4** and selected MurD residues for the D-Glu based interactions: (a) side chain oxygen of Thr321 and α-carboxylic oxygen of **1–4** (b) side chain nitrogen of Lys348 and α-carboxylic oxygen of **1–4** (c) backbone nitrogen of Ser415 and γ-carboxylic oxygen of **1–4** (d) side chain oxygen of Ser415 and γ-carboxylic oxygen of **1–4** (e) backbone nitrogen of Phe422 and γ-carboxylic oxygen of **1–4**

Compound	Thr321 (Å)	Lys348 (Å)	Ser415 (N) (Å)	Ser415 (O) (Å)	Phe422 (Å)
1[a]	4.3 ± 0.3	3.8 ± 0.3	2.9 ± 0.3	2.7 ± 0.3	3.1 ± 0.3
2	3.9 ± 0.4	2.8 ± 0.3	2.8 ± 0.1	2.6 ± 0.1	2.9 ± 0.2
3	3.1 ± 0.6	3.1 ± 0.7	2.9 ± 0.4	2.7 ± 0.3	3.0 ± 0.3
4	3.7 ± 0.5	2.9 ± 0.5	3.3 ± 0.7	3.0 ± 0.5	3.6 ± 0.8

For compound **4** the interactions with corresponding carboxylic acids are presumed

SD were calculated from four 5 ns MD production run simulations, which were initiated from four different starting configurations

[a] Data previously published in Ref. [15]

Table 2 The average distances between compounds **1–4** and selected MurD residues for the following monitored H-bond interactions: (a) ND1 nitrogen of His183 and oxygen of **1–4** amide or sulfonamide moiety (b) NE2 nitrogen of His183 and oxygen of **1–4** amide or sulfonamide moiety (c) backbone nitrogen of Thr36 and interacting moiety of compounds **1–4** (i) side chain oxygen of Thr36 and interacting moiety of compounds **1–4**

Compound	His183 (1) (Å)	His183 (2) (Å)	Thr36 (N) (Å)	Thr36 (O) (Å)
1[a]	3.6 ± 0.3	4.7 ± 0.3	–	–
2	3.7 ± 0.6	4.3 ± 0.3	3.4 ± 0.3	5.7 ± 0.3
3	3.8 ± 0.6	4.7 ± 0.6	3.6 ± 0.2	5.8 ± 0.3
4	4.3 ± 0.6	4.2 ± 0.3	3.9 ± 0.8	3.7 ± 0.6

SD were calculated from four 5 ns MD production run simulations, which were initiated from four different starting configurations

[a] Data previously published in Ref. [15]

obtained, in line with the experimentally observed distances, despite all crystal waters were omitted and a novel sphere of water molecules was constructed. Again, this behavior corroborated with the conclusions drawn in our previous study [15]. This shows that the H-bond interaction pattern is apparently conserved throughout the D-Glu-based inhibitor classes as in no case simulated so far a substantial deviation or instability was observed. This strongly conserved pattern of hydrogen bonds probably serves as a key anchor to adhere D-Glu based molecules firmly within the MurD substrate active site.

Next, distances between His183 and amide or sulfonamide moiety of inhibitors **2–4** were monitored (Table 2). Structural studies identified that this residue sometimes plays a role in the indirect hydrogen bond interaction mediated via a water molecule [14, 15, 18]. The obtained time dependent distance graphs between the closest lying sulfonamide or amide oxygen of the inhibitor **2–4** and His183 ND1 nitrogen are depicted in Fig. 6. Average lengths of this interaction ranged between 3.6 and 4.3 Å and suggested a potential role of His183 in optimal inhibitor recognition through indirect and/or direct interactions. This was also seen in MD trajectories in which the presence of both direct and water mediated interaction with His183 was observed. This reconfirmed potential importance of this residue for the inhibitor's MurD recognition. However, it has to be stressed that experimental QSAR of the known D-Glu based inhibitors showed that these interactions alone arising from D-Glu and sulfonamide or amide moieties were not sufficient for successful inhibition of the MurD enzyme activity [14–19].

Interestingly, the flexible biphenyl moiety of compounds **2–4** connected via a bridging flexible amino aliphatic spacer retained its twisted conformation during the MD simulations (see animation for compound **2** available in the Supplementary Material). This can be attributed to favorable stabilization of this moiety via hydrophobic interaction with Gly73, Leu416 (for the phenyl ring connected to the amide moiety) residues and Phe162 MurD residues (for the aminobenzylidene moiety). Comparable to its analogue from the *N*-sulfoamine-D-Glu series [15] compound **4** containing a naphthalene moiety displayed analogous behavior during the performed MD simulations. (See animation for compound **4** available in the Supplementary Material.) Overall, the lipophilic substituents attached to the D-Glu moiety are represented in almost all molecules which were found active when utilizing D-Glu drug design paradigm [14–18]. This indicates that hydrophobic interactions must play a vital role in binding as lack of these interactions resulted in complete loss of activity. Furthermore, this also pinpoints that the hydrogen bonds could serve primarily as anchors enabling subsequent hydrophobic interactions and to a less extent as the principal driving force of enzymatic inhibition in this case (see "Interaction energy analysis and binding free energies calculations" section for further discussion).

Inhibitors **2–4** contain structural elements, which by forming an additional H-bond interaction with Thr36 anchor the compounds firmly in the UMA binding site (Fig. 6) [14–18]. In the performed MD simulations 5-benzylidenethiazolidine-2,4-dione (compound 2) and 5-benzylidenethiazolidin-4-one moieties (compound 3) preserved a stable interaction between their carbonyl oxygen and backbone nitrogen of Thr36. Average distances of 3.4 ± 0.3 and 3.6 ± 0.2 Å were measured for this interaction respectively. Interactions of these moieties with side chain oxygen of Thr36 via thiazolidine nitrogen appear less favorable with observed distances of 5.7 ± 0.3 and 5.8 ± 0.3 Å. For compound **4** with 2-fluoro-4-cianobenzyl moiety the interactions of cyano nitrogen with side chain oxygen and backbone nitrogen of Thr36 were favorable showing distances of 3.9 ± 0.8 and 3.7 ± 0.8 Å, confirming a relatively stable hydrogen bond formation. SAR studies of the D-Glu-based series of MurD inhibitors simulated so far [15] resulted in an observation that Thr36 interaction in most cases does not substantially improve the binding affinity if the placement of the lipophilic moiety is already favorable [14]. To provide further insights into this subject the interaction energy analysis coupled with LIE free energy calculations was performed as discussed in the succeeding part of this study.

Interaction energy analysis and binding free energies calculations

Energetic aspect of the molecular recognition was first addressed by calculating interaction energies between ligands **2–4** and their surroundings (e.g. water, MurD protein, sodium ions) for both investigated states (free state and bound state) [22]. Time-dependence graphs of the interaction energy dissected into electrostatic and van der Waals energy terms for compounds **2–4** are depicted in Fig. 7 with energy values along with their partial differences gathered in Table 3. Calculated values of interaction energy terms of each simulation run for compounds **2–4** are available in the Supplementary material (Table **6S**) and do not deviate substantially from the overall average values discussed.

The initial analysis of the overall interaction energy values demonstrated that the binding of all analyzed compounds is energetically favored. Average values of the full interaction energy in the bound state comprised values: −525.5 kcal/mol (compound **2**), −532.3 kcal/mol (compound **3**), −503.3 kcal/mol (compound **4**) and in the free state the energy values −492.7 kcal/mol (compound **2**), −493.2 kcal/mol (compound **3**), −459.4 kcal/mol (compound **4**) were obtained, respectively. The interaction energy, as expected [15], fluctuated considerably and occupied relatively high energy values in both simulated states. This is not surprising since the investigated molecules possess two charged carboxylic groups [16–18].

In the interaction energy time-dependent diagrams (Fig. 7) the electrostatic and van der Waals components of the interaction energy were plotted separately. The van der Waals interaction energy fluctuated around the value of −20 kcal/mol in the free state and between values −40 and −60 kcal/mol in the bound state for compounds **2–4**. These observations show a clear preference of the van der Waals component for the bound state. This is in full agreement with our previous studies [15] (see values for the representative inhibitor **1** of the *N*-sulphonil MurD inhibitor series in Table 3).

The electrostatic component of the interaction energy of compound **2–4** fluctuated between −400 and −500 kcal/mol with mean value around −450 kcal/mol in both states (see Table 4). Interestingly, the average electrostatic interaction energy and the extent of its fluctuations are essentially identical in bound and in the free state for compounds **2–4** which can be further seen when both averages were subtracted (Table 3). With these observations an analogy with our previous study became is very apparent [15]. The electrostatic component represents the origin of significant fluctuations in the overall interaction energy; however the level of fluctuations was practically

Table 3 Average van der Waals and electrostatic interaction energies between D-Glu-based MurD inhibitors **1–4** and their surrounding (solvated receptor P or aqueous solution W) obtained from MD simulations

Compound	$\langle V_{L-P}^{vdW} \rangle$ (kcal/mol)	$\langle V_{L-W}^{vdW} \rangle$ (kcal/mol)	$\langle V_{L-P}^{vdW} \rangle - \langle V_{L-W}^{vdW} \rangle$ (kcal/mol)	$\langle V_{L-P}^{el} \rangle$ (kcal/mol)	$\langle V_{L-W}^{el} \rangle$ (kcal/mol)	$\langle V_{L-P}^{el} \rangle - \langle V_{L-W}^{el} \rangle$ (kcal/mol)
1[a]	−43.7 ± 0.5	−17.2 ± 0.1	−26.5 ± 3.4	−452.8 ± 1.2	447.7 ± 1.6	−5.1 ± 2.8
2	−51.1 ± 0.6	−19.5 ± 0.5	−31.6 ± 1.1	−474.4 ± 3.1	−473.2 ± 4.5	−1.2 ± 7.6
3	−56.2 ± 0.9	−21.9 ± 0.4	−34.3 ± 1.3	−476.1 ± 7.2	−471.3 ± 2.0	−4.8 ± 9.2
4	−58.4 ± 0.9	−24.9 ± 0.1	−33.5 ± 1.0	−444.9 ± 1.5	−434.5 ± 0.6	−10.4 ± 2.1

SD were calculated from four 5 ns MD production run simulations, which were initiated from four different starting configurations

[a] Data previously published in Ref. [15]

Table 4 Calculated binding free energies for the D-Glu-based MurD inhibitors **1–4** compared with the available experimental results [16–18] and relative energy differences

Compound	IC_{50} [μM]	$\Delta G_{binding}^{exp.}$ (kcal/mol)	$\Delta G_{binding}^{calc.}$ (kcal/mol)	Δ (kcal/mol)
1[a]	280	−4.9	−4.9 ± 0.3	0
2	85 ± 3	−5.5 ± 0.1	−5.6 ± 0.9	0.1
3	253 ± 27	−5.0 ± 0.1	−6.3 ± 0.6	1.3 (min 0.6)
4[b]	125	−5.3	−6.5 ± 0.3	1.2 (min 0.9)

The binding free energies were obtained using optimized empirical coefficients 0.175 (α) and 0.060 (β) [15]

SD were calculated from four 5 ns MD production run simulations, which were initiated from four different starting configurations

[a] Data previously published in Ref. [15]

[b] Determined Ki value [18]

Table 5 Decomposition of binding free energies for the D-Glu-based MurD inhibitors **1–4**

Compound	$\Delta G_{Moiety1}$ (kcal/mol)	$\Delta G_{Moiety2}$ (kcal/mol)	$\Delta G_{Moiety3}$ (kcal/mol)	$\Delta G_{Moiety4}$ (kcal/mol)
1[a]	−2.3 ± 0.5	−0.8 ± 0.1	−0.9 ± 0.1	−0.9 ± 0.1
2	−2.6 ± 0.3	−0.2 ± 0.2	−0.8 ± 0.1	−1.9 ± 0.1
3	−2.9 ± 0.3	−0.6 ± 0.2	−1.1 ± 0.1	−1.7 ± 0.2
4	−3.4 ± 0.3	−0.7 ± 0.1	−0.5 ± 0.1	−1.9 ± 0.2

The binding free energies of dissected moieties were obtained using optimized empirical coefficients 0.175 (α) and 0.060 (β) [15]

SD were calculated from four 5 ns MD production run simulations, which were initiated from four different starting configurations

[a] Data previously published in Ref. [15]

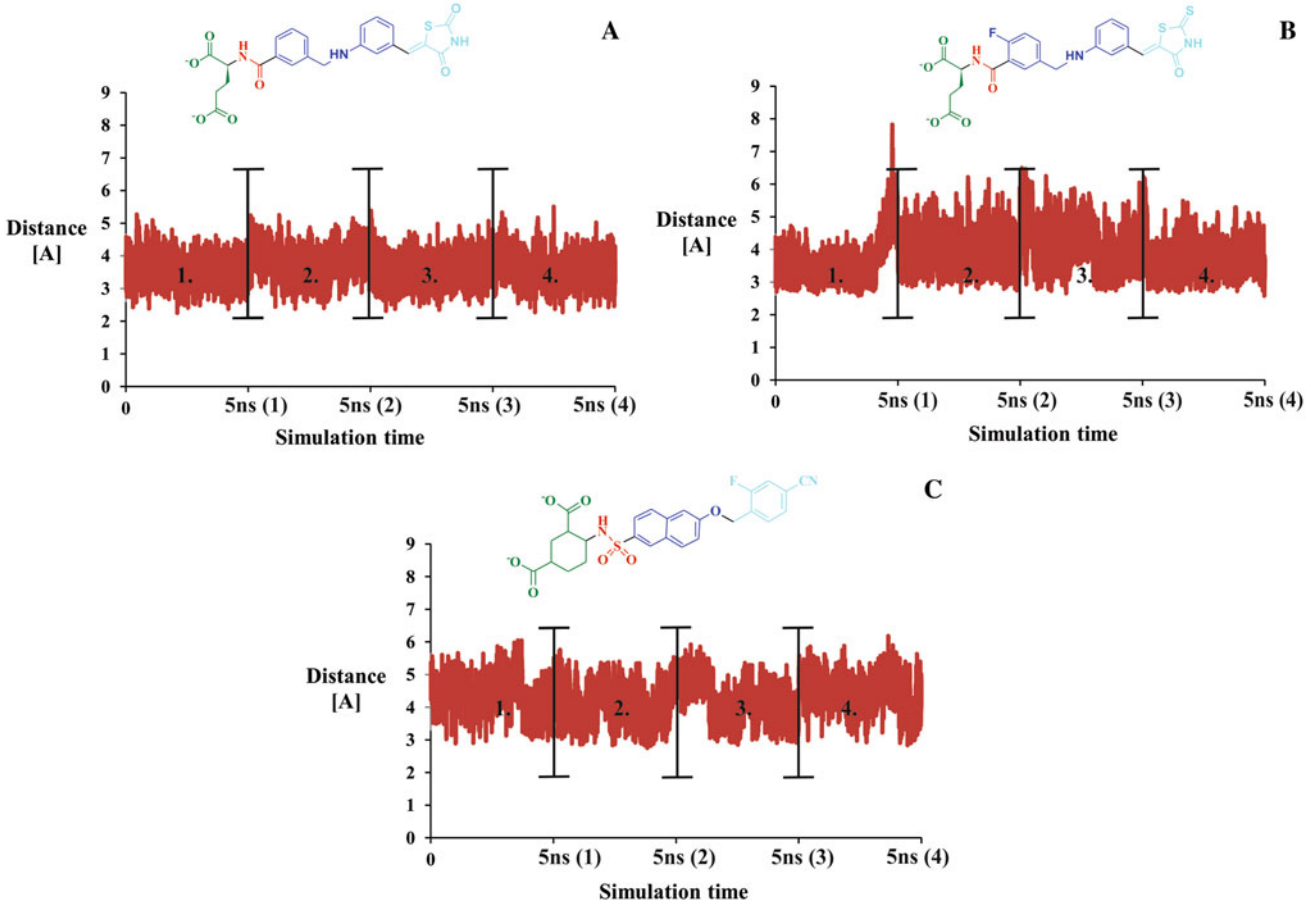

Fig. 6 Time-dependence of distance between ND1 nitrogen of His183 and nearest oxygen of the sulfonamide moiety in compound **2** (**a**) and **3** (**b**) or amide oxygen in compound **4** (**c**). *Bars* indicate boundaries between four 5 ns MD production runs staring from four different starting configurations

identical in both states (in water and in the active site of the enzyme) for all compounds. Thus, the electrostatics of ligands **2–4** behaves analogously to *N*-sulfonamide D-Glu series [15]. The van der Waals component of binding suggests that a favorable placement of these interactions is one of the general prerequisites for the inhibitory activity of D-Glu based compounds.

Our goal in the previous free energy study of the D-Glu inhibitors was to derive the LIE coefficients that could be further applicable to similar series of MurD inhibitors [15]. In this way LIE equation could be used for a larger set of diverse molecules within the D-Glu drug design paradigm thus providing a strong support to the static molecular docking scoring function assessments. Since in the present study all simulations are firmly based on the experimental structural data the binding free energies of investigated inhibitors **2–4** were calculated using optimized empirical coefficients 0.176 (α) and 0.060 (β) of the LIE equation (3)

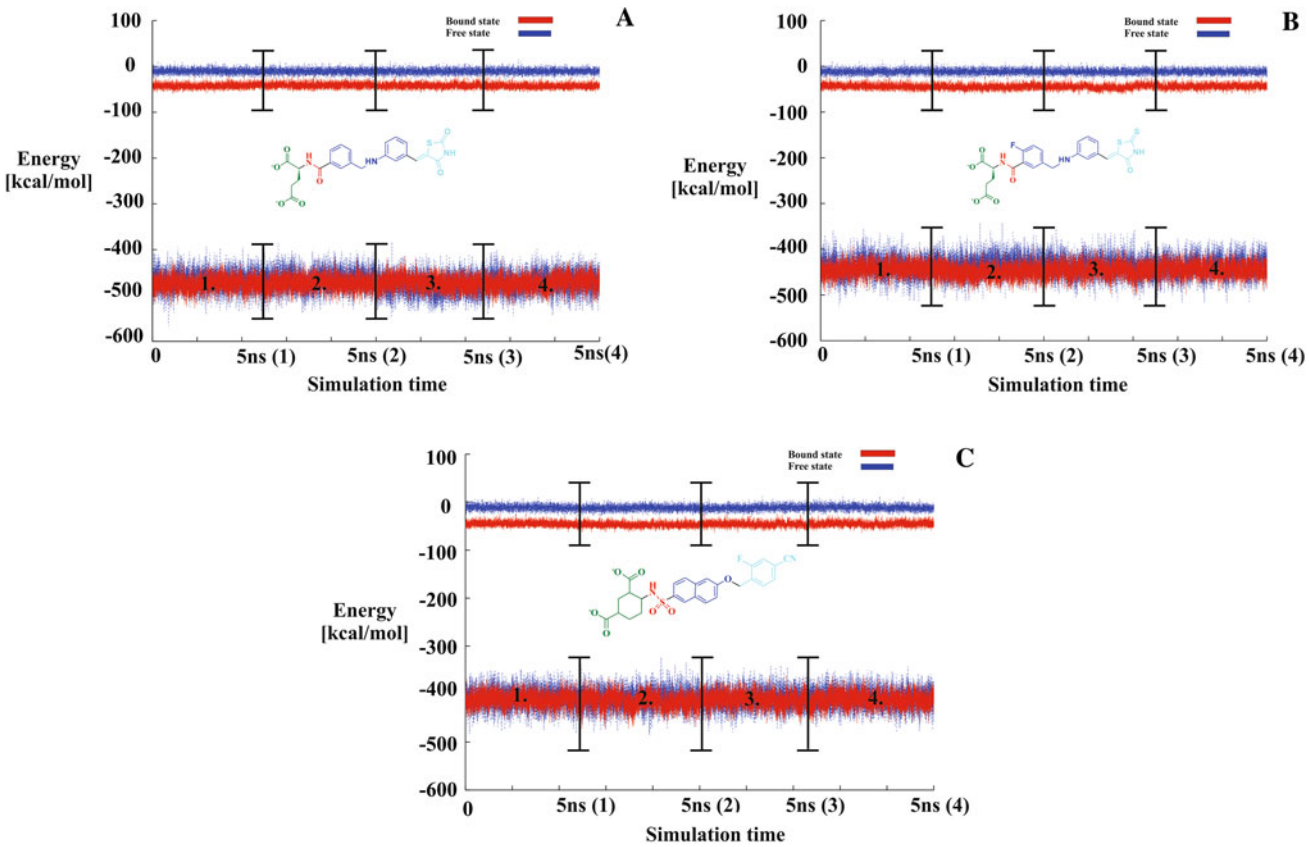

Fig. 7 Interaction energy between compounds **2** (**a**), **3** (**b**), **4** (**c**) and its surrounding [water and sodium ions in the free state (*blue*) and water, sodium ions and protein in the bound state (*red*)] during the 20 ns MD simulation dissected into van der Waals (above) and electrostatic (below) interaction energy during the 20 ns MD simulation. *Bars* indicate boundaries between four 5 ns MD production runs staring from four different starting configurations

developed in our initial LIE study. The obtained values of binding free energies are assembled in Table 4 along with their experimental counterparts for comparison and relative differences are provided in the final column of Table 4. Our previous steady-state kinetics experiments revealed that IC_{50} values of D-Glu based inhibitors (e.g. compound **1**) were in a good agreement with the measured Ki values [14]. Thus, the obtained IC_{50} values represent a good first approximation of the Ki value and for compounds **2** and **3** Ki was estimated by their IC_{50} values. In addition, in the novel studied series rigid compound **4** displayed the same correlation between these two parameters [18]. Experimental binding free energies of compounds were calculated by the standard thermodynamic relation $\Delta G_{binding} = RT \ln (Ki)$ where R, T and Ki represent a universal gas constant, thermodynamic temperature and experimental dissociation constant, respectively.

The utilization of the previously derived LIE coefficients yielded the value of -5.6 ± 0.9 kcal/mol for the D-Glu derivative **2** containing a 5-benzylidenethiazolidin-2,4-one moiety whereas the experimental binding free energy of compound **2** was determined to be -5.5 ± 0.1 kcal/mol, which is in agreement with experimental data. The 5-benzylidenethiazolidin-2,4-one D-Glu derivative (**3**) displayed an experimental binding free energy of -5.0 ± 0.1 kcal/mol while the mean calculated LIE estimate was slightly higher at -6.3 ± 0.6 kcal with a free energy difference of 1.3 kcal/mol, minimal difference if taking the SD into account amounted to 0.6 kcal/mol. Compounds **2** and **3** contain a rhodanine moiety that can represent a source of non-specific (promiscuous) inhibition in in vitro assays [37–39]. In all performed in vitro inhibition assays of these compounds they were assayed according to standard recommendations to avoid this potential issue [16–18].

Similarly, the observed experimental binding energy of -5.3 kcal/mol for the rigid sulphonamide compound **4** was approximately 1 kcal/mol away from the calculated value of -6.5 ± 0.6 kcal/mol. Overall, results of LIE calculations were predicted within 1 kcal/mol difference indicating a reasonable transferability of the determined LIE coefficients to novel molecules designed within the D-Glu paradigm. Correct ranking order of compounds **2**–**4** in terms of binding free energy values was unfortunately not

achieved. The main reason for this is a fairly small difference between binding free energies of the inhibitors under study. Current force fields are not sufficiently accurate to achieve the level of accuracy required to rank order such compounds and much longer simulation times would be required to achieve such high precision results.

Linear interaction energy methodology also enables decomposition of binding free energy into contributions arising from different moieties of a molecule under investigation. For drug design purposes this is particularly favorable since the allocation of binding free energy contributions to specific moieties is especially important for generating new guidelines in the optimization phase of the drug discovery cycle. However, a caveat must be stated that due to complex nature of molecular recognition process different contributions to the overall binding can behave in a highly nonadditive fashion [40–42]. As in our previous study binding contributions of the lipophilic tail of the *N*-sulphonyl-D-Glu inhibitors allowed for discrimination between the inhibitors and showed additional correlation with experimental values [15] we opted to proceed with this analysis also in this study.

Calculated partial binding free energies for dissected moieties of compounds **2**–**4** are presented in Table 5. Division scheme and obtained average interactions energy values of all decomposed moieties of compounds **2**–**4** are available in the Supplementary material (Tables **7S.1**–**7S.3**–**10S.1**–**10S.3**). Energy values within each individual MD simulation did not deviate substantially from the overall average values discussed. The calculated binding free energy of the D-glutamic acid moiety without nitrogen atom varied within a small interval between -2.6 ± 0.3 and -2.9 ± 0.3 kcal/mol for both derivatives **2** and **3**, making a substantial contribution to the overall binding energy. The binding free energy of the rigid bicarboxylic analogue was even more favorable with calculated binding value of -3.4 ± 0.3 kcal/mol. This increase can be partially contributed to the increased ability of a larger cyclohexane ring in **4** to form more hydrophobic interactions with hydrophobic residues located within the D-Glu binding pocket compared to the smaller aliphatic part of the D-Glu moiety.

The binding free energy of the amide moiety was found to be -0.2 ± 0.2 kcal/mol (compound **2**) and -0.6 ± 0.2 kcal/mol (compound **3**) and can be compared to sulfonamide moiety in the rigidized compound **4** (-0.7 ± 0.1 kcal/mol). The energy contribution of the naphthalene moiety of **4** with included bridging oxygen was found to be -0.5 ± 0.1 kcal/mol. Replacement of the naphthalene moiety present in compounds **1** and **4** by a biphenyl system included in compounds **2** and **3** connected via an aliphatic chain afforded analogous binding affinities of -0.8 ± 0.1 and -1.1 ± 0.1 kcal/mol respectively. The introduction of a fluorine atom on the first phenyl ring in compound **3** improved the binding affinity by 0.3 kcal/mol in comparison to a biphenyl contribution of compound **2**.

The second most important binding contribution to the overall binding was found to be 5-benzylidenethiazolidin-2,4-dione (compound **2**) or the 5-benzylidenethiazolidine-2-one (compound **3**) scaffold which contribute to binding with -1.9 ± 0.1 and -1.7 ± 0.2 kcal/mol respectively. Interestingly, in our previous study an in silico compound (not yet synthesized) with incorporated 2H-1,3-thiazine-2,6(3H)-dione group which is structurally similar to benzylidenethiazolidine series yielded a favorable affinity of -1.2 ± 0.6 kcal/mol [15–18]. Binding free energy of the lipophilic tail of compound **4** was found to be -1.9 ± 0.2 kcal/mol showing that incorporation of the 4-cyano 2-fluoro-phenyl group provides a valuable source of binding free energy while the incorporation of fluorine additionally strengthens the interactions compared to unsubsituted derivatives [15].

Study of the MurD inhibitors using static drug design techniques and optimization guidelines

To further support our observations obtained by the molecular dynamics studies an established drug design tool, GRID program, was exploited to investigate the MurD binding site. This program enables the identification of energetically favorable binding sites on macromolecular targets [43]. In our case, hydrophobic interactions and hydrogen bond acceptors (D-Glu functionality recognition and interactions with Thr36) that were shown to play a decisive role for successful inhibition were investigated [15–18]. All crystal structures of our treated ligands 2XPC, 2Y68 and 2X50 as well as 2JFF crystal structure of the compound **1** completely overlapped with virtually non-existent RMSD differences (see Supplementary material for the structures overlay) Thus, a representative 2JFF crystal structure was used as an input structure for the GRID program and representative energy contours are presented in Fig. 8 [43]. It has to be noted that identical results were obtained when other available MurD crystal structures were used. Calculated GRID contour surfaces of the dry probe at -0.5 kcal/mol and hydrogen bond acceptor oxygen (O) probe at -4.5 kcal/mol in the MurD binding site are presented in Fig. 8a, b. At least three favorable hydrophobic regions were identified by GRID. One region occupies the space in the D-Glu binding site giving further evidence of the usefulness of introduction of the rigid dicarboxyllic moiety [18, 19]. A second region is located between the binding space of the sulfonamide/amide and lipophilic part (naphthalene or phenyl) of these compounds and a third small region is located in the uridine part of the substrate binding pocket. Available QSAR results indicate that interaction with all three hydrophobic

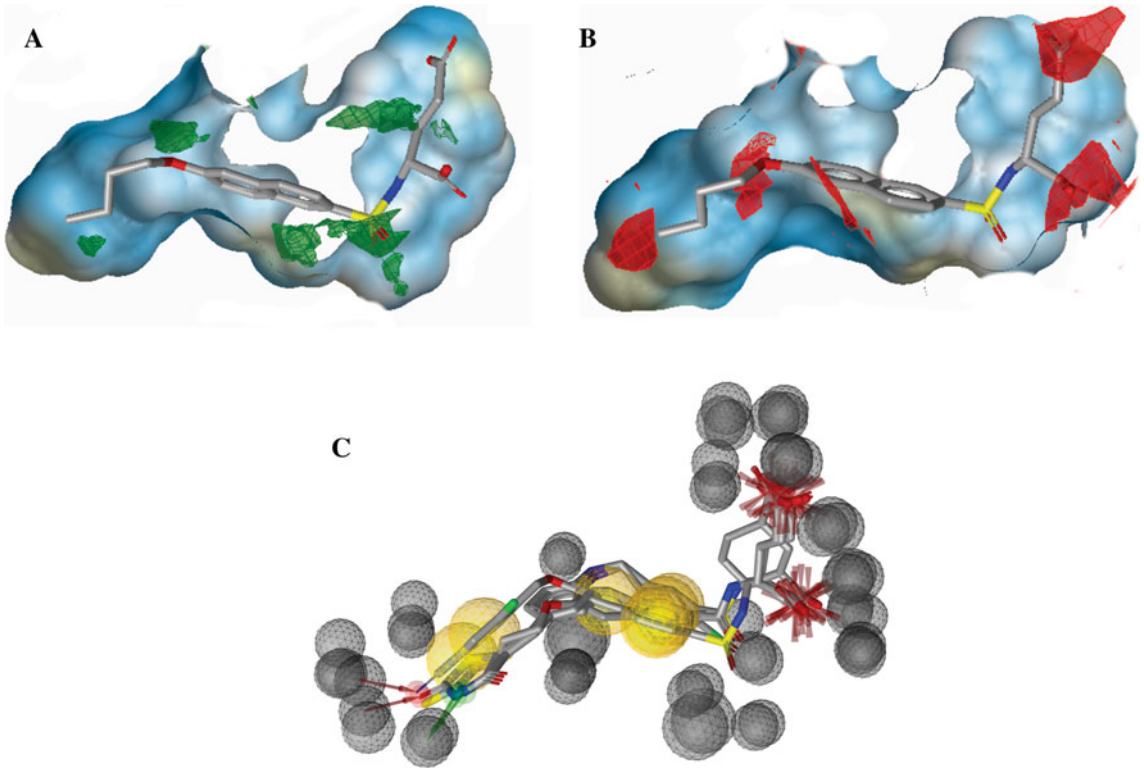

Fig. 8 Calculated GRID contour surfaces of the **a** dry probe (*green*) at −0.5 kcal/mol and **b** hydrogen bond acceptor oxygen (O) probe (*red*) at −4.5 kcal/mol in the MurD binding site. Compound **1** from the 2JJF crystal structure is indicated for better visualization of the favorable locations of both probes [14]. **c** Aligned derived structure-based pharmacophores of compounds **1**–**4** within their corresponding crystal structures. The *green arrow* represents the hydrogen bond donor, the *red arrow* the hydrogen bond acceptor, a *red sphere* is a negative ionizable group, *yellow spheres* denote hydrophobic features and *gray spheres* depicted exclusion volume spheres

areas is necessary for molecular recognition [16–18]. In compounds **2**–**4** the phenyl moiety (**4**) or the sulfur atom of the benzylidenethiazolidine ring (**2**, **3**) occupy this area.

The GRID oxygen probe isolated regions within the binding site favorable for hydrogen acceptor interaction. From the GRID contour surface using oxygen probe at −4.5 kcal/mol can clearly be seen that two regions where carboxylic acid functionalities are located and the space where Thr36 interaction takes place represent the most favorable areas for hydrogen acceptor interaction. In addition, a small area located around oxygen connecting the naphthalene part was observed where interaction with Arg 37 can be formed. We also calculated a GRID map by using water probe (GRID map available in the Supplementary material Figure **7S**). As observed in the structural studies [14, 16–18] the extensive MurD binding site is occupied by numerous water molecules. The calculated GRID water map corroborated this observation. As numerous water molecules must be displaced during the ligand binding entropic contributions or even domain movement observed for MurD enzyme [9–11] could play an important role in overall binding free energy outcome [44].

The LigandScout program [45] is an established structure-based pharmacophore generator and was used to explore the molecular recognition of bound ligands **1**–**4** taking the surrounding macromolecular environment into account. In Fig. 8c aligned [46] derived structure-based pharmacophores of compounds **1**–**4** from the 2XPC, 2Y68, 2X50 and 2JFF crystal structures are presented and the gray spheres depicted exclusion volume spheres which correspond to the spatial constraints imposed by the MurD binding site and conserved water molecules [14–16, 18]. In all molecules **1**–**4** two negative ionizable areas were identified that reflect the negatively charged electrostatic features of the carboxylic groups. Two hydrophobic interaction areas occupy approximate position of the hydrophobic interaction identified by GRID maps. Furthermore, the hydrogen bond interaction with Thr 36 showed its importance in molecular recognition of these compound classes.

The performed static and dynamic investigations of novel classes of MurD inhibitors provided several useful guidelines that could be used proficiently in further efforts to optimize both inhibitor classes. Potential changes are outlined schematically in Fig. 9 and we clustered the

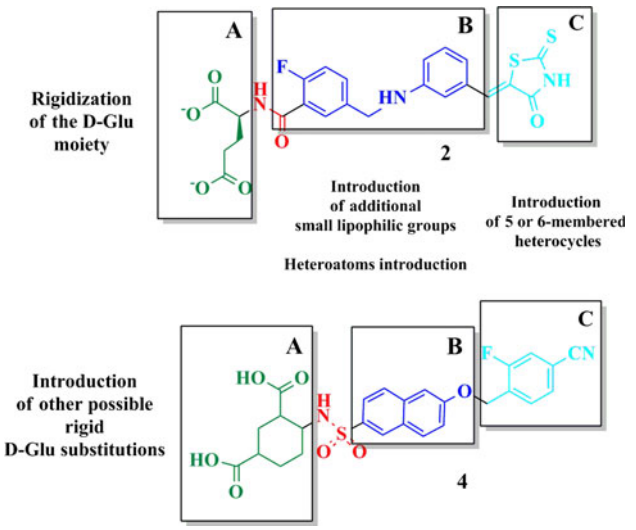

Fig. 9 Guidelines for further optimization of discovered MurD inhibitor classes **2** and **4** based on the LIE results

guidelines in three structural parts a–c. In part A we took into account the observed more favorable binding contribution of the rigidized cyclohexene D-Glu moiety (3.4 ± 0.3 kcal/mol) in comparison to the initial D-Glu moiety (between 2.3 and 2.9 kcal/mol). This observation suggests that introduction of the rigid D-Glu scaffolds such as, benzene and different heterocyclic 6-membered rings (saturated on non-saturated) with appropriately positioned dicarboxyilic moieties would yield compounds with improved MurD inhibition activity and should be included in further optimization of both series. In part b we consider LIE-determined binding energy contributions of the central lipophilic moiety (between 0.5 and 1.1 kcal/mol) and GRID calculations. These results point out that substitutions introduced on different positions of the biphenyl or naphthalene moiety preferably halogen atoms and small lipophilic substituents (e.g.methyl and ethyl methoxy) would contribute favorable to binding free energy. The strategy of incorporating groups on the lipophilic core has already showed some initial promising results [16, 17] and should be according to LIE calculations pursued further. In addition, in our previous LIE study it was shown that naphthalene moiety can be transformed into a heterocyclic moiety (e.g. 4-methylquinazoline) and retain favorable partial binding affinity contribution [15] confirming possible introductions of heteroatoms (nitrogen, oxygen) in the lipophilic core. For the part c, LIE calculations have revealed that proper placement of this moiety is important for the inhibitory activity as it contributes between 1 and 2 kcal/mol to the overall binding affinity (Table 5). Improvements of this part could include substitution of the benzylidenethiazolidine or ciano-benzene moiety with different five or six membered heterocycles (nitrogen or oxygen-based) with either preserved free nitrogen or ciano mimicking functionality important for the Thr36 interaction.

Conclusions

In our investigation of the MurD bacterial target we studied two recently discovered classes of the MurD ligase inhibitors resulting from the lead optimization [16–18] of the *N*-sulfonamide D-Glu inhibitors by taking the available experimental structural data into account. Analysis of the MD trajectories confirmed a stable network of hydrogen bonds that enable a proper orientation of the ligands in the MurD active site as well as proper positioning of the compounds' hydrophobic parts. Application of the LIE coefficients determined previously for the *N*-sulfonamide D-Glu inhibitors [15] to the calculated average interaction energies of compounds **2–4** yielded good estimates of binding free energies for these inhibitors. A prevailing role of non-polar van der Waals interactions as the main driving force of binding was determined—an observation present in all classes of D-Glu based inhibitors of MurD discovered to date.

The ability to exactly dissect the free energy into components arising from different groups of atoms or types of interactions within the LIE formalism enabled explicit evaluation of contributions important for successful inhibitory activity. In particular, the interaction of compound moieties in two hydrophobic areas of the MurD binding site along with the favorable enhancement of the hydrophobicity in the D-Glu binding pocket by a D-Glu rigidization represent the cornerstones that should be considered in further molecular design. Some potential optimization guidelines based on these novel observations were outlined for both synthetic routes. These results provide valuable information in support of the D-Glu paradigm of MurD ligase inhibition, which has contributed to an improved molecular understanding of this family of bacterial enzymes.

Supplementary material

(1) Structural alignment of MurD crystal structures with inhibitors **1–4**, (2) Outline of the LIE study of novel D-Glu-based MurD ligase inhibitors, (3) Scheme of the thermodynamic cycle applied in the LIE method, (4) Calculated RESP partial atomic charges and atom types of derivatives **2–4**, (5) Decomposition schemes for simulated ligands **2–4**, (6) Average distances of compounds **2–4** for each MD simulation, (7) Average interactions energy values of compounds **2–4** for each MD simulation, (8) Average

interactions energy values of the decomposed moieties of compounds **2–4** for each MD simulation (9) The time dependence of all distances monitored diring the MD simulations for compounds **2–4**, (10) Calculated GRID contour surfaces for the water probe. (11) Animations presenting the bound state of compound **2** and **4** during the MD simulation.

Acknowledgments This work was supported by the postdoctoral grant of the Ministry of Higher Education, Science and Technology of the Republic of Slovenia (Grant Number: Z1-4111).The authors would like thank Dr. Jernej Zidar and Barbara Pogorelčnik from the National institute of Chemistry, Slovenia, for their helpful technical assistance and Dr. Yasmin Aristei from Molecular Discovery Ltd. for GRID map calculations. Dr. Urban Bren from the National Institute of Chemistry, Ljubljana is acknowledged for introducing us to LIE methodology in our previous binding study of MurD inhibitors.

References

1. Rice LB (2006) Unmet medical needs in antibacterial therapy. Biochem Pharmacol 71:991–995
2. Brown ED, Wright GD (2005) New targets and screening approaches in antimicrobial drug discovery. Chem Rev 105:759–774
3. Vollmer W, Blanot D, de Pedro MA (2008) Peptidoglycan structure and architecture. FEMS Microbiol Rev 32:149–167
4. Smith CS (2006) Structure, function and dynamics in the *mur* family of bacterial cell wall ligases. J Mol Biol 362:640–655
5. Bertrand JA, Auger G, Martin L, Fanchon E, Blanot D, Le Beller D, van Heijenoort J, Dideberg O (1999) Determination of the MurD mechanism through crystallographic analysis of enzyme complexes. J Mol Biol 289:579–590
6. Anderson MS, Eveland SS, Onishi H, Pompliano DL (1996) Kinetic mechanism of the Escherichia coli UDPMurNAc-tripeptide D-alanyl-D-alanine-adding enzyme: use of a glutathione *S*-transferase fusion. Biochemistry 35:16264–16269
7. Emanuele JJ Jr, Jin H, Yanchunas J Jr, Villafranca JJ (1997) Evaluation of the kinetic mechanism of Escherichia coli uridine diphosphate-*N*-acetylmuramate:L-alanine ligase. Biochemistry 36:7264–7271
8. Perdih A, Hodoscek M, Solmajer T (2009) MurD ligase from *E. coli*: Tetrahedral intermediate formation study by hybrid quantum mechanical/molecular mechanical replica path method. Proteins: Struct Funct Bioinf 74:744–759
9. Bertrand JA, Fanchon E, Martin L, Chantalat L, Auger G, Blanot D, van Heijenoort J, Dideberg O (2000) "Open" structures of MurD: domain movements and structural similarities with folylpolyglutamate synthetase. J Mol Biol 301:1257–1266
10. Perdih A, Kotnik M, Hodoscek M, Solmajer T (2007) Targeted molecular dynamics simulation studies of binding and conformational changes in *E. Coli* MurD. Proteins: Struct Funct Bioinf 68:243–254
11. Perdih A, Solmajer T (2012) MurD ligase from *E. coli*: C-terminal domain closing motion. Comput Theor Chem 979:73–81
12. Zoeiby AE, Sanschagrin F, Levesque RC (2002) Structure and function of the Mur enzymes: development of novel inhibitors. Mol Microbiol 47:1–12
13. Tanner ME, Vaganay S, van Heijenoort J, Blanot D (1996) Phosphinate inhibitors of the D-glutamic acid-adding enzyme of peptidoglycan biosynthesis. J Org Chem 61:1756–1760
14. Kotnik M, Humljan J, Contreras-Martel C, Oblak M, Kristan K, Hervé M, Blanot D, Urleb U, Gobec S, Dessen A, Solmajer T (2007) Structural and functional characterization of enantiomeric glutamic acid derivatives as potential transition state analogue inhibitors of MurD ligase. J Mol Biol 370:107–115
15. Perdih A, Bren U, Solmajer T (2009) Binding free-energy calculations of *N*-sulphonyl glutamic acid inhibitors of MurD ligase. J Mol Model 15:983–996
16. Zidar N, Tomasic T, Sink R, Rupnik V, Kovac A, Turk S, Patin D, Blanot D, Contreras Martel C, Dessen A, Müller Premru M, Zega A, Gobec S, Peterlin Masic L, Kikelj D (2010) Discovery of novel 5-benzylidenerhodanine and 5-benzylidenethiazolidine-2,4-dione inhibitors of MurD ligase. J Med Chem 53:6584–6594
17. Tomašić T, Zidar N, Šink R, Kovač A, Blanot D, Contreras-Martel C, Dessen A, Müller-Premru M, Zega A, Gobec S, Kikelj D, Peterlin Mašič L (2011) Structure-based design of a new series of D-glutamic acid based inhibitors of bacterial UDP-*N*-acetylmuramoyl-L-alanine:D-glutamate ligase (MurD). J Med Chem 54:4600–4610
18. Sosič I, Barreteau H, Simčič M, Sink R, Cesar J, Zega A, Grdadolnik SG, Contreras-Martel C, Dessen A, Amoroso A, Joris B, Blanot D, Gobec S (2011) Second-generation sulphonamide inhibitors of D-glutamic acid-adding enzyme: activity optimisation with conformationally rigid analogues of D-glutamic acid. Eur J Med Chem 46:2880–2894
19. Perdih A, Kovač A, Wolber G, Blanot D, Gobec S, Solmajer T (2009) Discovery of novel benzene 1,3-dicarboxylic acid inhibitors of bacterial MurD and MurE ligases by structure-based virtual screening approach. Bioorg Med Chem Lett 19:2668–2673
20. Åqvist J, Medina C, Samuelson JE (1994) A new method for predicting binding affinity in computer-aided drug design. Protein Eng 7:385–391
21. Åqvist J, Luzhkov VB, Brandsdal BO (2002) Ligand binding affinities from MD simulations. Acc Chem Res 35:358–365
22. Marelius J, Kolmodin K, Feierberg I, Åqvist J (1998) A molecular dynamics program for free energy calculations and empirical valence bond simulations in biomolecular systems. J Mol Graph Model 16:213–225
23. Cornell WD, Cieplak P, Bayly CI, Gould IR, Merz M Jr, Ferguson DM, Spellmeyer DC, Fox T, Caldwell JW, Kollman PA (1995) A second generation force field for the simulation of proteins, nucleic acids, and organic molecules. J Am Chem Soc 117:5179–5197
24. Gaussian 09, Revision A.1, Frisch MJ, Trucks GW, Schlegel HB, Scuseria GE, Robb MA, Cheeseman JR, Scalmani G, Barone V, Mennucci B, Petersson GA, Nakatsuji H, Caricato M, Li X, Hratchian HP, Izmaylov AF, Bloino J, Zheng G, Sonnenberg JL, Hada M, Ehara M, Toyota K, Fukuda R, Hasegawa J, Ishida M, Nakajima T, Honda Y, Kitao O, Nakai H, Vreven T, Montgomery JA Jr, Peralta JE, Ogliaro F, Bearpark M, Heyd JJ, Brothers E, Kudin KN, Staroverov VN, Kobayashi R, Normand J, Raghavachari K, Rendell A, Burant JC, Iyengar SS, Tomasi J, Cossi M, Rega N, Millam JM, Klene M, Knox JE, Cross JB, Bakken V, Adamo C, Jaramillo J, Gomperts R, Stratmann RE, Yazyev O, Austin AJ, Cammi R, Pomelli C, Ochterski JW, Martin RL, Morokuma K, Zakrzewski VG, Voth GA, Salvador P, Dannenberg JJ, Dapprich S, Daniels AD, Farkas Ö, Foresman JB, Ortiz JV, Cioslowski J, Fox DJ, Gaussian, Inc., Wallingford CT, 2009
25. Bayly CI, Cieplak P, Cornell WD, Kollman PA (1993) A well-behaved electrostatic potential based method using charge restrains for deriving atomic charges: the RESP model. J Phys Chem 97:10269–10280
26. Jorgensen WL, Chandrasekhar J, Madura JD, Impey RW, Klein ML (1983) Comparison of simple potential functions for simulating liquid water. J Chem Phys 79:926–935

27. King G, Warshel A (1989) A surface constrained all-atom solvent model for effective simulations of polar solutions. J Chem Phys 91:3647–3661
28. Lee FS, Warshel A (1992) A local reaction field method for fast evaluation of long-range electrostatic interactions in molecular simulations. J Chem Phys 97:3100–3107
29. Handler N, Brunhofer G, Studenik C, Leisser K, Jaeger W, Parth S, Erker T (2007) 'Bridged' stilbene derivatives as selective cyclooxygenase-1 inhibitors. Bioorg Med Chem 15:6109–6118
30. Humphrey W, Dalke A, Schulten K (1996) VMD: visual molecular dynamics. J Mol Graph 14:33–38
31. Christ CD, Mark AE, van Gunsteren WF (2010) Basic ingredients of free energy calculations: a review. J Comput Chem 31:1569–1582
32. Chen X, Tropsha A (2006) Calculation of the relative binding affinity of enzyme inhibitors using the generalized linear response method. J Chem Theory Comput 2:1435–1443
33. Carlson J, Boukharta L, Aquist J (2008) Combining docking, molecular dynamics and the linear interaction energy method to predict binding modes and affinities for non-nucleoside inhibitors to HIV-1 reverse transcriptase. J Med Chem 51:2648–2656
34. Kolb P, Huang D, Dey F, Caflisch A (2008) Discovery of kinase inhibitors by high-throughput docking and scoring based on a transferable linear interaction energy model. J Med Chem 51:1179–1188
35. Bortolato A, Moro S (2007) In silico binding free energy predictability by using the linear interaction energy (LIE) method: bromobenzimidazole CK2 inhibitors as a case study. J Chem Inf Model 47:572–582
36. Bren M, Florián J, Mavri J, Bren U (2007) Do all pieces make a whole? Thiele cumulants and the free energy decomposition. Theor Chem Acc 117:535–540
37. Baell JB, Holloway GA (2010) New substructure filters for removal of pan assay interference compounds (PAINS) from screening libraries and for their exclusion in bioassays. J Med Chem 53:2719–2740
38. Mendgen T, Steuer C, Klein CD (2011) Privileged scaffolds or promiscuous binders—a comparative study on rhodanines and related heterocycles in medicinal chemistry. J Med Chem 55:743–753
39. McGovern SL, Stoichet BK (2003) Kinase inhibitors: not just for kinases anymore. J Med Chem 46:1478–1783
40. Baum B, Muley L, Smolinski M, Heine A, Hangauer D, Klebe G (2010) Non-additivity of functional group contributions in protein-ligand binding: a comprehensive study by crystallography and isothermal titration calorimetry. J Mol Biol 397:1042–1054
41. Patel Y, Gillet VJ, Howe T, Pastor J, Oyarzabal J, Willett P (2008) Assessment of additive/nonadditive effects in structure-activity relationships: implications for iterative drug design. J Med Chem 51:7552–7562
42. Kuhn B, Fuchs JE, Reutlinger M, Stahl M, Taylor NR (2011) Rationalizing tight ligand binding through cooperative interaction networks. J Chem Inf Model 51:3180–3198
43. Goodford PJ (1985) A computational procedure for determining energetically favorable binding sites on biologically important macromolecules. J Med Chem 28:857–864
44. Kollman PA (1993) Free energy calculations: applications to chemical and biochemical phenomena. Chem Rev 93:2395–2417
45. Wolber G, Langer T (2005) LigandScout: 3-D pharmacophores derived from protein-bound ligands and their use as virtual screening filters. J Chem Inf Model 45:160–169
46. Wolber G, Dornhofer A, Langer T (2006) Efficient overlay of small organic molecules using 3D pharmacophores. J Comput Aided Mol Design 20:773–788